

Generating X-ray lines from annihilating dark matter

Emilian Dudas^{a,*}, Lucien Heurtier^{a,†} and Yann Mambrini^{b,‡}

^a *CPhT, Ecole Polytechnique, 91128 Palaiseau Cedex, France* and

^b *Laboratoire de Physique Théorique, Université Paris-Sud, F-91405 Orsay, France*

We propose different scenarios where a keV dark matter annihilates to produce a monochromatic signal. The process is generated through the exchange of a light scalar of mass of order 300 keV - 50 MeV coupling to photon through loops or higher dimensional operators. For natural values of the couplings and scales, the model can generate a gamma-ray line which can fit with the recently identified 3.5 keV X-ray line.

I. INTRODUCTION

Physics community is still in the quest of the dominant matter component in the Universe. Even if we know quite well the cosmological abundance of this dark matter [1, 2], little is known about its mass and couplings. In view of recent results from both direct and indirect detection experiments, the Weakly Interacting Massive Particle (WIMP) paradigm, corresponding to a ~ 100 GeV particle interacting weakly with the visible sector begins to be severely constrained by XENON [3], LUX [4] or FERMI satellite [5]. On the other hand, several other scenarios offer much lighter [9] or heavier [10] candidates with feeble [6, 7] or very feeble [8] couplings. Their thermal histories are relatively different (but not less motivated) from the standard freeze out one. The cases of FIMP (for Freeze In Massive Particle or Feebly Interacting Massive Particle) or WISP (for Weakly Interacting Slim Particle) are typical cases where the coupling is too weak to reach the thermal equilibrium with the standard model bath [6]. The dark matter candidate can be so weakly coupled that it decoupled from the bath at the reheating epoch, like the gravitino or candidates motivated by SO(10) schemes. Other scenario proposed an even more weakly interacting particle, so weakly interacting that the dark matter is stable at the scale of the age of the universe: the decaying dark matter (see [11] for a review on the subject).

At present, clues for the presence of an interacting dark matter are rare. However, recently a 3.55 keV X-ray line has been reported in the stacks analysis of 73 galaxy clusters from the XMM-Newton telescope [12] with a significance larger than 3σ . A similar analysis finds evidence at the 4.4σ level for a 3.52 keV line from their analysis of the X-ray spectrum of the Andromeda galaxy (M31) and the Perseus Cluster [13]. In both analysis, the unidentified line was interpreted as a possible signal of sterile neutrino dark matter ν_s [14] decaying through a loop $\nu_s \rightarrow \gamma\nu$.

While more conventional explanations in term of atomic physics effects are currently lacking, several works have been released in the following weeks, all focussing on a decaying dark matter candidate. Extensions with a sterile neutrino as dark matter candidate [15], axions or ALPs [16], axinos [17], pseudo-Nambu-Goldstone bosons [18] or supersymmetric models (gravitino [19], sgoldstino [20] or low scale supersymmetry breaking [21]) were proposed, all relying on processes ensuring a fine tuned lifetime $\tau \simeq 10^{28}$ seconds to fit the observed line. Other more exotic candidates like decaying moduli [22], millicharged dark matter [23], dark atoms¹ [24], magnetic dark matter [26], majoron decay [27] or multicomponent [28] have been proposed. Another original model was studied in [29, 30] with an eXciting dark matter, where the photons come from the transition from an excited state down to the ground state for the dark matter particle, which in this case can be significantly heavier than 3.5 keV. Moreover, it is well known that for a warm dark matter candidate of mass $\sim \text{keV}$, free streaming produces a cutoff in the linear fluctuation power spectrum at a scale corresponding to dwarf galaxies and can fit observations for $m_s \gtrsim 1.5 \text{ keV}$ [31].

All of these scenarios seem to exclude (maybe too early) an annihilating dark matter scenario [32]. Indeed, the cross section needed to fit the excess measured in [12, 13] is $\sigma v \simeq 10^{-33} \text{ cm}^3\text{s}^{-1}$ which corresponds to an effective scale Λ of $\Lambda \simeq 10 \text{ GeV}$ for a 3.5 keV dark matter, in the classical effective operators approach. This scale is too low to be due to heavy particles charged under the electromagnetic field.

In this work however, we show that such cross section arises naturally when we go beyond the naive effective operators approach and consider microscopic constructions with the presence of a light hidden mediator coupling to the standard model through effective operators. Such approach had been explored in the case of a vector boson or a heavy fermionic mediator [36] but did not consider the possibility of a scalar one. Furthermore these studies had worked out a lower bound on the dark matter mass of order $\mathcal{O}(\text{MeV})$ in order to fit both ray fluxes

* emilian.dudas@cphpt.polytechnique.fr

† lucien.heurtier@cphpt.polytechnique.fr

‡ yann.mambrini@th.u-psud.fr

¹ For an introduction to the subject, see e.g. [25]

and relic density measurements [37]. We will show that this bound can actually be overcome if one considers the dark sector to be living in a thermal bath of temperature differing from the one of the visible sector.

The paper is organized as follows. After a summary of the effective operators approach in the next section, we describe our model in Section III and extract the parameter space allowed to fit the observed X-ray line. We then compute the relic abundance predicted in this restricted parameter space by adding an additional coupling of the mediator to a light sterile right-handed neutrino in Section IV. We show that the model can fit WMAP/PLANCK data taking into account that the bath of the hidden sector is at a different temperature compared to the standard model one. We then conclude in section V with an explicit example of an UV model, before giving the relevant technical formulae in the appendix in the case of a fermionic dark matter.

II. THE FAILURE OF A NAIVE EFFECTIVE OPERATORS APPROACH

A. A priori

Since Fermi's time the classical way to explain a signal or to work out predictions at a scale beyond the standard model one² (which is the one that one can reach experimentally at a given time) is to use the effective operators approach. Indeed, it seems natural to imagine that the physics beyond a measurable scale of energy is represented by heavy particles not yet produced in accelerators, but coupling to the observable sector. This is frequently used in LHC studies [38] or dark matter searches [39]. However, it is obvious that this effective operators approach has its limitations. First of all, the coupling to the visible sector generated by loops of heavy states can be highly dependent on the hidden microscopic physics (gauge or Yukawa-like couplings) but, more dramatically, the presence of light states modifies considerably the predictions, as was shown in [40]. Supersymmetric or grand unified models do not escape this rule: light stau or Z' for instance generate new processes observable at LHC and not predicted by a naive effective operators approach. This is exactly what is happening in the case of a cosmological monochromatic signal as one discusses below.

B. The monochromatic signal

If the signal analysed in [12, 13] is generated by dark matter annihilation to two photons $ss \rightarrow \gamma\gamma$ (with a dark matter mass of 3.5 keV) then one should fit the annihilation cross section $\langle\sigma v\rangle_{\gamma\gamma}$ with the flux measured in the vicinity of the sun. A naive estimate of the total luminosity of Perseus can be computed using

$$L = \int_0^{R_{Pe}} 4\pi r^2 n_{DM}^2 \langle\sigma v\rangle_{\gamma\gamma} = \int_0^{R_{Pe}} 4\pi r^2 \left(\frac{\rho(r)}{m_s}\right)^2 \langle\sigma v\rangle_{\gamma\gamma} \quad (1)$$

with R_{pe} is the Perseus radius. As a first approximation, one can consider like in [33] a mean density of dark matter in the cluster. The Perseus observation involved a mass³ of $M_{Pe} = 1.49 \times 10^{14} M_\odot$ in a region of $R_{Pe} = 0.25$ Mpc at a distance of $D_{Pe} = 78$ Mpc from the solar system. One can then estimate

$$\begin{aligned} n_{DM} &\simeq \frac{1.49 \times 10^{14} M_\odot}{m_s} \frac{3}{4\pi R_{Pe}^3} = 2.0 \times 10^{-37} \text{GeV}^3 \\ &= 2.6 \times 10^4 \text{cm}^{-3} . \end{aligned} \quad (2)$$

Combining Eq.(1) and (2), one can compute the luminosity in the Perseus cluster,

$$L \simeq 1.2 \times 10^{55} \left(\frac{3.5 \text{ keV}}{m_s}\right)^2 \left(\frac{\langle\sigma v\rangle_{\gamma\gamma}}{10^{-26} \text{cm}^3 \text{s}^{-1}}\right) \text{ ph/s} . \quad (3)$$

One can then deduce the flux $\phi_{\gamma\gamma} = L/(4\pi D_{Pe}^2)$ that one should observe on earth

$$\phi_{\gamma\gamma} = 1.7 \times 10^{-5} \left(\frac{3.5 \text{ keV}}{m_s}\right)^2 \left(\frac{\langle\sigma v\rangle_{\gamma\gamma}}{10^{-32} \text{cm}^3 \text{s}^{-1}}\right) \text{ cm}^{-2} \text{s}^{-1} \quad (4)$$

The cumulative flux of $\phi_{\gamma\gamma} \sim 4 \times 10^{-6} \text{cm}^{-2} \text{s}^{-1}$ from [12] is hard to interpret in the dark matter framework as it arises from a combination of clusters at a variety of distances. However, according to the authors of [13, 29], one can identify a monochromatic signal arising from M31 or Perseus cluster with a flux $\phi_{\gamma\gamma} = 5.2_{-2.13}^{+3.70} \times 10^{-5}$ photons cm^{-2} per seconds at 3.56 keV with the cluster core. One can make a more refined analysis, considering for instance a more complex halo structure like Einasto or NFW profile as in [29] but the result will not change

² The "standard model scale" varying with time: $\simeq \text{MeV}$ in 1897, $\simeq \text{GeV}$ in 1932, $\simeq 100 \text{ GeV}$ in 1983, TeV scale nowadays.

³ See table 2 of [12]

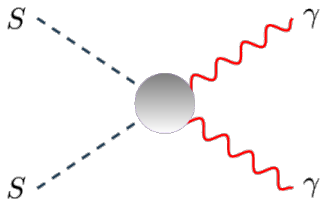


FIG. 1. Effective diagram for dark matter annihilation

dramatically⁴. One could also look at the Centaurus observation like in [33] with $M_{Ce} = 6.3 \times 10^{13} M_{\odot}$ and a radius of $R_{Ce} = 0.17$ Mpc.

Finally, taking into account also other observations like M31, we will impose in our analysis a conservative required annihilation cross section estimated as

$$\langle \sigma v \rangle_{\gamma\gamma} \simeq (2 \times 10^{-33} - 4 \times 10^{-32}) \text{ cm}^3 \text{ s}^{-1}. \quad (5)$$

However, for such a light dark matter particle annihilating into photons, it is important to check the consequences of injecting secondary particles on the recombination, leaving an imprint on Cosmic Microwave Background (CMB) anisotropies. The authors of [34] show that the corresponding condition is given by

$$\langle \sigma v \rangle_{\gamma\gamma}^{CMB} \lesssim 2.42 \times 10^{-27} \left(\frac{m_s}{1 \text{ GeV}} \right) \text{ cm}^3 \text{ s}^{-1}, \quad (6)$$

which for a 3.5 keV dark matter is $\langle \sigma v \rangle_{\gamma\gamma} < 8.5 \times 10^{-33} \text{ cm}^3 \text{ s}^{-1}$. *In fine* one will then restrict oneself to the parameter space allowing a monochromatic signal and respecting the CMB constraints:

$$2 \times 10^{-33} \text{ cm}^3 \text{ s}^{-1} < \langle \sigma v \rangle_{\gamma\gamma} < 8.5 \times 10^{-33} \text{ cm}^3 \text{ s}^{-1}. \quad (7)$$

C. A posteriori

In the case of a scalar particle annihilating into two photons, the CP-even effective lagrangian can be written⁵

$$\mathcal{L}_{eff} = \frac{S^2}{\Lambda^2} F_{\mu\nu} F^{\mu\nu}, \quad (8)$$

⁴ We thank M. Yu. Khlopov for having drawn our attention to ref. [35] for a detailed analysis on profiles concerning gamma ray production from so called dark matter clumps

⁵ To simplify the analysis, we will consider a scalar dark matter candidate with CP-even couplings thorough the paper. The other cases (fermionic dark matter, CP-odd or pseudo-scalar couplings..) change our conclusion by factors of order of unity and are treated in appendix.

with $F_{\mu\nu} = \partial_\mu A_\nu - \partial_\nu A_\mu$ being the electromagnetic field strength. The scale Λ is related to the mass of the particles running in the loops (see Fig.(1)) which, being charged under $U(1)_{em}$, should be heavier or at least of the order of TeV. A list of generic couplings of this type can be found in [41]. We will write in the appendix the results we obtained in other cases.

It is important to notice that such a light dark matter can contribute to the effective number of neutrinos N_{eff} . However, it has been shown recently that a dark matter annihilating into photons in sub-MeV masses is possible only in the case of a scalar dark matter [42]. Such processes have already been computed in [43] and one obtains

$$\langle \sigma v \rangle_{\gamma\gamma}^{eff} = \frac{2m_s^2}{\pi\Lambda^4}. \quad (9)$$

Applying the constraints (7) to the annihilation cross section (9) one obtains

$$10 \text{ GeV} < \Lambda < 15 \text{ GeV}. \quad (10)$$

This value is obviously far below any accelerator limit on charged particles. It seems then impossible to UV complete this operator and achieve a large enough rate. However, as we will see below, the effective operators approach cannot be applied anymore when the UV sector contains light states.

III. A NATURAL MICROSCOPIC APPROACH

It is then natural to build a microscopic model and to see how observables are modified. But natural in which sense? Natural in the sense that the presence of a keV-MeV dark matter particle *naturally* leads to a keV scale dynamics, as the presence of GeV particles in the standard model naturally leads to GeV scale dynamics in the Higgs sector. We then can suppose the presence of a (pseudo)scalar coupling to the dark matter candidate, and generating the keV dynamics. The simplest way to generate such dynamics is through a "higgs-like" portal. We will consider by simplicity a scalar dark matter; other dark matter spin or couplings do not change our conclusions and are treated in the appendix.

A. The scalar model

We will work in the framework of a scalar portal ϕ , coupling directly at tree-level to dark matter, but indirectly to the standard model through loops. This is a typical secluded dark matter type of model [44]. The lagrangian can then be written for a scalar dark matter

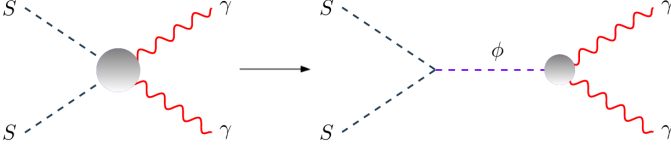


FIG. 2. Microscopic diagram for dark matter annihilation

$$\mathcal{L}_{eff} \supset -\frac{m_s^2}{2} S^2 - \frac{m_\phi^2}{2} \phi^2 - \tilde{m} \phi S^2 + \frac{\phi}{\Lambda} F_{\mu\nu} F^{\mu\nu}. \quad (11)$$

We assume the parameter \tilde{m} to be a free mass scale parameter. However such coupling can be explicitly generated by symmetry breaking in renormalizable models, as illustrated in section V. In the latter case, \tilde{m} is expected to be at most of the same order of magnitude than m_ϕ since it gets its value from the *vev* of a field $\Phi = v_\phi + \phi$ after spontaneous symmetry breaking. Furthermore this is what would be more generally expected if \tilde{m} is generated by whatever dynamical mechanism involving only ϕ and the light field S . The mass scale Λ is related to the mass of heavy particles integrated in the loop. In a perturbative set up with N charged fermions running in the loop $\Lambda \sim \frac{4\pi}{N h_\phi \alpha} M_\psi$, where h_ϕ is the Yukawa coupling of ϕ to the charged fermions of mass M_ψ . Using the constraint $M_\psi \gtrsim 500$ GeV from collider searches and perturbativity one finds that the minimum natural values for Λ are $\Lambda \sim 50 - 500$ TeV, whereas $\Lambda \sim 5$ TeV can only be obtained in a strongly coupled hidden sector.

Such a lagrangian gives for the annihilation cross section (process depicted in Fig.(2))

$$\langle \sigma v \rangle_{\gamma\gamma}^{micro} = \frac{4m_s^2 \tilde{m}^2}{\pi \Lambda^2 (4m_s^2 - m_\phi^2)^2}. \quad (12)$$

B. X-ray line

Depending on the hierarchy between the masses of the mediator ϕ and the dark matter particle S , the condition (7) leads to two kinds of constraints :

Case A : $m_\phi \gtrsim m_s$ (Heavy Mediator),

$$m_\phi \simeq (12.3 - 17.6) \sqrt{\frac{m_s}{3.5 \text{ keV}}} \sqrt{\frac{\tilde{m}}{\Lambda}} \text{ GeV} \quad (13)$$

Case B : $m_\phi \lesssim m_s$ (Light Mediator),

$$\frac{\tilde{m}}{\Lambda} \sim (1.63 - 3.36) \times 10^{-13}. \quad (14)$$

Both cases give at first sight viable results. One can understand easily why it is so in the microscopic approach compared to the effective operators approach of Eq.(9). Indeed, as recently emphasized by the authors of [40] for the LHC analysis of mono jet events, the effective operators approach ceases to be valid once the ultraviolet (microscopic) theory contains some light mediators, which is exactly our case. This comes from two powers less in Λ in the computation of observables: heavier states become now reasonably heavy compared to the result Eq.(10).

We will see however that experimental bounds on light scalar particle interactions with the electromagnetic sector are strongly restrictive.

C. Experimental Bounds

As we just mentioned above, interactions of a light scalar, or axion-like particle (ALP) with the visible sector is very much constrained by collider data (LEP) and astrophysics. Indeed bounds on pseudoscalar particles interacting with photons (see [46]) have been studied, using LEP data from ALEPH, OPAL, L3 and DELPHI, and shown that the coupling of the pseudoscalar with photons cannot exceed a value of $2.6 \times 10^{-4} \text{ GeV}^{-1}$ for a mediator of mass $m_\phi \lesssim 50$ MeV, which means, in terms of our mass scale

$$\Lambda \gtrsim 3 \text{ TeV} \quad [m_\phi \lesssim 50 \text{ MeV}]. \quad (15)$$

Furthermore, one of the most restrictive constraints on ALPs comes from the non-observation of anomalous energy loss of horizontal branch (HB) stars via a too important ALP production [47]. Indeed those constraints impose

$$\Lambda \gtrsim 10^{10} \text{ GeV} \quad [m_\phi \lesssim 30 \text{ keV}], \quad (16)$$

for a mediator mass up to $m_\phi \lesssim 30$ keV. At higher masses arise constraints coming from the CMB and BBN studies, setting lower limits on the coupling with photons. A nice review on the subject can be found in [48, 49]. Various astrophysical constraints on ALP mass and coupling to photons are summarized in, e.g. [50].

These constraints on our model essentially put lower bounds on Λ . Indeed, for a light mediator (Case B) HB experiments impose that the mass scale Λ takes very high values ($\gtrsim 10^{10}$ GeV). In this case, as indicated by Eq.(14), one would need the tri-linear coupling to be of order $\tilde{m} \gtrsim 10^{-3}$ GeV. However, in this case, since m_ϕ is assumed to be smaller than the keV scale, one would conclude that $\tilde{m}/m_\phi \gtrsim 10^3$ which is, as mentioned in the previous section, quite unnatural. We will then concentrate our study on Case A, where the mediator ϕ is assumed to be heavier than the dark matter field S .

In Case A, the discussion is a bit more subtle, as far as the experimental constraints are concerned. For mediator masses lower than a hundred keV, the mass scale Λ must reach very high values ($\gtrsim 10^{16}$ GeV) to escape experimental exclusion bounds. Still such region of the parameter space is not acceptable since it would lead to a very heavy parameter \tilde{m} . Then for higher masses of the mediator ($m_\phi \gtrsim 300$ keV) more reasonable values of Λ are allowed, and we are left with lower bounds coming from LEP (mentioned above) and upper bounds on Λ arising from CMB dilution and BBN perturbations. Different choices of Λ will then lead to different pairs of (m_ϕ, \tilde{m}) , as depicted in Fig.(3)

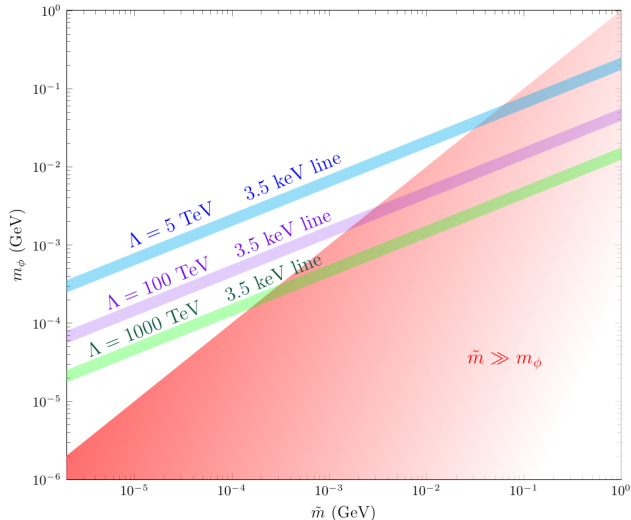


FIG. 3. (m_ϕ, \tilde{m}) parameter space allowed by the γ flux measurements in the case of a heavy mediator (Case A), for different values of Λ . The red shaded region indicates where \tilde{m} is higher than m_ϕ .

In order to fix ideas, and anticipating results of section V, we indicated in red in the figure the region where $\tilde{m} \gtrsim m_\phi$. This shows clearly, that imposing $m_\phi \gtrsim 300$ keV sets an upper limit for Λ , giving approximately

$$\Lambda \lesssim 1000 \text{ TeV}. \quad (17)$$

Furthermore, the lower limit $\Lambda \gtrsim 5$ TeV mentioned in section III A – still acceptable if there is some strongly coupled hidden sector generating the effective mass scale Λ – imposes an upper limit on the mediator mass, $m_\phi \lesssim 50$ MeV⁶. One would thus expect from this model that the mediator mass lies in the region

$$300 \text{ keV} \lesssim m_\phi \lesssim 50 \text{ MeV}. \quad (18)$$

⁶ As mentioned in previous sections, assuming that the effective coupling between the mediator ϕ and the photons comes from some perutrative heavy physics sets a stronger limit on Λ leading to masses of the mediator $m_\phi \lesssim 5$ MeV.

IV. RELIC ABUNDANCE

A. State of the art

Computing the relic abundance in models with a very weak annihilation cross section and a keV dark matter particle is highly non-standard. Indeed, it is well known from the standard lore that a hot dark matter candidate leads to a relic density

$$\Omega h^2 \simeq 9.6 \times 10^{-2} \frac{g_{eff}}{g_s(x_f)} \left(\frac{m_s}{1 \text{ eV}} \right), \quad (19)$$

where g_{eff} is the effective number of degrees of freedom of the dark matter candidate and g_s the effective number of degrees of freedom for the entropy. Eq.(19) gives $m_s \simeq 5$ eV if one wants to respect PLANCK [2] limit $\Omega_{DM} h^2 = 0.1199 \pm 0.0027$. However, this condition is valid only under the hypothesis that the dark matter is in thermal equilibrium with a common temperature T with the thermal bath. In the case of the line signal observed in the clusters, the cross section necessary to fit the result is far below the classical thermic one $\langle \sigma v \rangle_{therm} = 3 \times 10^{-26} \text{ cm}^3 \text{ s}^{-1}$. This idea had led previous studies to rule out scalar dark matter candidates lighter than $\mathcal{O}(\text{MeV})$ [37]. In fact, the dark bath, composed of the light mediator ϕ and the dark matter S cannot be in equilibrium with the standard plasma.

There are several ways to address this issue. A first possible attempt to solve the problem, proposed in [6] and [7], is to suppose that the dark matter is produced through the *freeze in* mechanism: the interacting photons annihilate to produce the dark matter in the inverse process of Fig.(2). Yet it is not possible to get the right relic density in this way since, solving the Boltzmann equation in this case would produce too much dark matter. Indeed equilibrium dark matter density would reach quickly a value that would overclose the Universe.

Another way to solve the problem was proposed in [54, 55] where the authors noticed that the condition (19) is not valid anymore if the temperature of the hidden sector T_h is different from the one of the thermal bath T . In this case, one can compute the temperature T_h needed to obtain a 3.56 keV particle respecting the relic abundance constraint. Yet, as we will see in what follows, we still need the hidden sector content to be richer in order to provide new dark matter annihilation channels leading to the right relic abundance. This will be done adding to the model a right-handed sterile neutrino.

B. Dark matter annihilation into sterile neutrinos

One way of solving the lack of annihilation of dark matter described above is to assume that a right-handed sterile neutrino couples directly to the mediator scalar particle

previously introduced. This would provide another channel for annihilating dark matter which would boost the relic density to its experimental value.

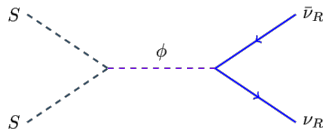


FIG. 4. Microscopic model of dark matter decaying into right-handed sterile neutrinos.

In a similar fashion than in section III A, one can add to the usual neutrino interaction terms a Yukawa coupling between the field ϕ and the sterile neutrino ν_R ⁷

$$-\mathcal{L}_\nu = \frac{M}{2}\nu_R\nu_R + m_D\nu_L\nu_R + \lambda_\nu\phi\nu_R\nu_R + h.c., \quad (20)$$

After diagonalization of the mass matrix, the sterile neutrino gets mass $m_{st} \simeq M$ while the active one obtains a mass of $m_{act} \simeq m_D^2/M$ via the seesaw mechanism. Such interactions give the following cross section for dark matter annihilation into a pair of sterile neutrinos

$$\langle\sigma v\rangle_{\nu\nu} = \frac{\lambda_\nu^2 \tilde{m}^2}{8\pi^2} \frac{(m_s^2 - M^2)}{m_s^2(4m_s^2 - m_\phi^2)^2} \sqrt{1 - \frac{M^2}{m_s^2}}. \quad (21)$$

Assuming that M is negligible compared to m_s leads to a cross section depending only on m_s , m_ϕ and \tilde{m} , λ_ν :

$$\langle\sigma v\rangle_{\nu\nu} \sim \frac{\lambda_\nu^2}{8\pi^2} \left(\frac{\tilde{m}}{m_s}\right)^2 \frac{m_s^2}{(4m_s^2 - m_\phi^2)^2}. \quad (22)$$

C. Cosmological constraints on a hidden sector

In such a framework, dark matter and sterile neutrinos can be seen as living together in a *hidden* thermal bath decoupled from the visible sector. Its temperature can be denoted by

$$T_h \equiv \xi(t)T, \quad (23)$$

where in what follows ξ is assumed to be a constant parameter⁸. As described in [54, 55], such a point of view can have important consequences on the thermal dynamics of the hidden sector, since ξ enters into the Boltzmann equation. Indeed dark matter can decouple while still relativistic or semi-relativistic and lead to different relic densities, as the parameter ξ takes different values

(See Fig.(6)). Such freedom in the temperature of the hidden sector is yet constrained by astrophysical considerations. In particular, a hidden sector dark matter can freeze out while still being relativistic. It is then important to check that its free streaming length is smaller than typical galactic length scales so that it does not destroy the matter power spectrum. Another constraint, introduced by Tremaine and Gunn in [56], comes from bounding the phase-space density of structures like small dwarf galaxies by statistical quantum mechanics considerations. Both constraints are computed and summarized in the case of a ~ 3 keV dark matter in [54] and lead naturally to a relic density value different from the one of the visible thermal bath ($\langle\sigma v\rangle_0 \sim 10^{-9}$ GeV⁻²), depending on how cold the hidden sector is. We thus get

$$0.015 \langle\sigma v\rangle_0 \lesssim \langle\sigma v\rangle \lesssim 0.045 \langle\sigma v\rangle_0, \quad (24)$$

the upper limit corresponding to the free streaming constraint whereas the lower one to a strict Tremaine-Gunn bound. One should also remark that the dark matter is relatively warm ($x_f = m_s/T_f \simeq 2 - 4$ for points respecting WMAP/PLANCK) in this case. As a warm candidate, it can elude the classical issues of cold dark matter *i.e.* the few number of galaxy mergers ($\lesssim 10\%$) or the core observed profiles compared to the cusp ones predicted by N-body simulations.

D. Results

In the light of section III C and equation (22) one can now constrain couplings between the mediator ϕ to both the dark and the visible sector \tilde{m} and λ_ν , taking into account that relic density can lie in the region (24) exhibited in the previous section, as well as imposing constraints on the photons flux measurement. Results are presented in Fig.(5) where we show the allowed parameter space imposing cosmological bounds [54] superimposed within the regions fitting the 3.5 keV excess, for $m_\phi = 500$ keV. As one can see, a relatively large region respects the cosmological bounds and the monochromatic excess. The values of λ_ν are also quite constrained ($\sim 10^{-7} - 10^{-5}$, depending on the mass scale Λ), leading to different values of the hidden sector temperature (as represented in Fig.(6)). Furthermore it could be interesting in a future work to combine our analysis with neutrino bounds.

V. AN EXPLICIT UV MODEL

We give here an explicit example realizing the case A of Section III. The model contains a scalar σ and a pseudoscalar S , together with a (set of) fermion(s) ψ , with the lagrangian

$$\mathcal{L} = \mathcal{L}_{kin} + \frac{\mu^2}{2}(\sigma^2 + S^2) - \frac{\lambda}{4}(\sigma^2 + S^2)^2$$

⁷ We use two-component spinor notation in this equation.

⁸ See ref. [55] for a discussion on the validity of this approximation.

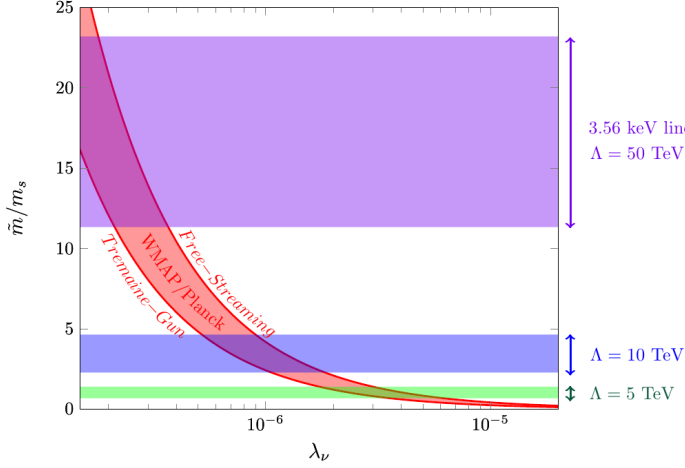


FIG. 5. Constraints on the parameter space (\tilde{m}, λ_ν) , for $m_\phi = 500$ keV; considering cosmological constraints (relic abundance, free streaming and Tremaine-Gunn bounds) in the red/dark band and a 3.5 keV excess (blue/green region) for different values of the BSM scale Λ (see the text for details).

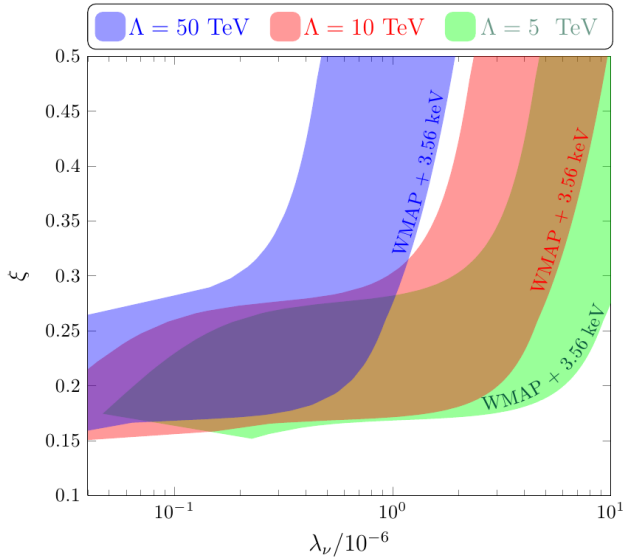


FIG. 6. Hidden temperature factor ξ allowed by the flux measurement limits, as a function of the relic density value, for different values of the mass scale Λ .

$$-\bar{\psi}(h_1\sigma + ih_2S\gamma_5)\psi + \frac{\sigma}{\Lambda}F_{\mu\nu}F^{\mu\nu}. \quad (25)$$

The set of fermions ψ are part of the hidden sector, in particular they are singlets with respect to the Standard Model. By defining the complex field $\Phi = \frac{1}{\sqrt{2}}(\sigma + iS)$, we can split the lagrangian (25) into two parts:

$$\begin{aligned} \mathcal{L} &= \mathcal{L}_0 + \mathcal{L}_1, \text{ where} \\ \mathcal{L}_0 &= \mathcal{L}_{kin} + \mu^2\Phi^\dagger\Phi - \lambda(\Phi^\dagger\Phi)^2 - (h_1\bar{\psi}_L\Phi\psi_R + \text{h.c.}), \\ \mathcal{L}_1 &= i(h_1 - h_2) S \bar{\psi}\gamma_5\psi + \frac{\sigma}{\Lambda}F_{\mu\nu}F^{\mu\nu}. \end{aligned} \quad (26)$$

Notice that the whole lagrangian is invariant under the vectorial transformation

$$U(1)_V : \quad \psi \rightarrow e^{i\alpha}\psi, \quad \Phi \rightarrow \Phi, \quad (27)$$

whereas \mathcal{L}_0 is also invariant under the axial transformation

$$U(1)_A : \quad \psi \rightarrow e^{i\beta\gamma_5}\psi, \quad \Phi \rightarrow e^{-2i\beta}\Phi. \quad (28)$$

The axial transformation is broken by \mathcal{L}_1 and is therefore an exact symmetry of the hidden sector lagrangian in the limit $h_1 = h_2$. The symmetry is broken additionally by the coupling to the photons. At tree-level, S is massless since it is the (pseudo)Goldstone boson of the axial $U(1)_A$ symmetry. For $\mu^2 > 0$ there is a symmetry breaking vacuum, with $\langle\sigma\rangle = v$ and $v^2 = \frac{\mu^2}{\lambda}$. By expanding around the minimum one also finds at tree-level

$$m_\phi^2 = 2\mu^2, \quad \tilde{m} = \sqrt{\frac{\lambda}{2}} m_\phi. \quad (29)$$

At the one-loop level, there is a quantum correction to the potential $V_1 = V_1(h_1^2\sigma^2 + h_2^2S^2)$, which generates a mass for the pseudo-goldstone boson S , proportional to $m_S^2 \sim O(\frac{h_2^2 - h_1^2}{16\pi^2})m_\phi^2$, which has a one-loop suppression with respect to the mediator mass ϕ . This model is an example of a UV embedding of case A of Section III, in which one naturally expects $\tilde{m} \leq m_\phi$ and selects therefore natural regions in the parameter space in Section III.

CONCLUSIONS

In this work, we have shown that a keV scalar dark matter can be the main constituent of the matter of the universe, producing monochromatic X-ray signals that can be fitted with the recently claimed events of a 3.5 keV line in nearby clusters of galaxies. Moreover, we know that for a warm dark matter mass of order of a keV, free streaming produces a cutoff in the linear fluctuation power spectrum at a scale corresponding to dwarf galaxies and can fit observations for $m_s \gtrsim 1.5$ keV [31]. We have shown that astrophysical, collider and relic density constraints are more difficult to accommodate. They are however possible to satisfy for certain values of the mediator mass m_ϕ and scale Λ of the couplings between the mediator and the photon $300 \text{ keV} \lesssim m_\phi \lesssim 50 \text{ MeV}$ and $5 \text{ TeV} \lesssim \Lambda \lesssim 1000 \text{ TeV}$. These values can conversely be considered as a prediction of our setup of keV dark matter models leading to X-ray monochromatic lines. We also showed that as pointed out recently by [40], the study of *pure* effective models – as it is often done in the literature – misses important quantitative effects. Indeed, we could reach a cross section in agreement with the analysis of XMM Newton data only through the building of a microscopic model and the exchange of a

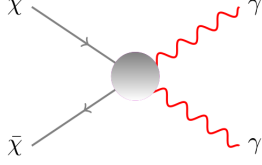


FIG. 7. Effective diagram for dark matter annihilation in the fermionic case

light scalar. Finally, it should be interesting to look at the observability of such a light meson. This task is far beyond the scope of our paper but is under investigation.

Acknowledgements. The authors would like to thank M. Goodsell and A. Ringwald for very useful discussions. E.D. and L.H. would like to thank the Alexander von Humboldt foundation and DESY-Hamburg for support and hospitality during the final stage of the project and Y.M. would like to thank K. Tarachenko for constant support. This work was supported by the French ANR TAPDMS **ANR-09-JCJC-0146**, the Spanish MICINN's Consolider-Ingenio 2010 Programme under grant Multi-Dark **CSD2009-00064**, the European Union FP7 ITN INVISIBLES (Marie Curie Actions, PITN- GA-2011- 289442) and the ERC advanced grants MassTeV and Higgs@LHC.

APPENDIX

For completeness, we present in this appendix the main alternatives to the Lagrangian (11). They do not affect however our conclusions.

Fermionic dark matter

Effective operator approach

With the same philosophy used in section II, we could consider a fermionic dark matter χ interacting with photons through effective operators of the form

$$\frac{\bar{\chi}\chi}{\Lambda^3} F_{\mu\nu} F^{\mu\nu}, \quad \frac{\bar{\chi}\gamma_5\chi}{\Lambda^3} F_{\mu\nu} \tilde{F}^{\mu\nu}, \quad (30)$$

where $\tilde{F}^{\mu\nu} = \frac{1}{2}\epsilon^{\mu\nu\rho\sigma}F_{\rho\sigma}$. The obtained cross sections are, respectively

$$\langle\sigma v\rangle_{\gamma\gamma}^{eff} = \frac{8m_\chi^4 v^2}{\pi\Lambda^6}, \quad \frac{8m_\chi^4}{\pi\Lambda^6}. \quad (31)$$

The constraints (7) give then

$$0.061 < \Lambda < 0.078 \quad , \quad 0.091 < \Lambda < 0.12 \quad (\text{GeV}) \quad (32)$$

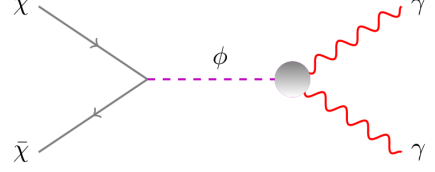


FIG. 8. Microscopic diagram for dark matter annihilation in the fermionic case

It is clear then that in the fermionic case these values are even more incompatible with experimental constraints coming from colliders.

Microscopic Model

Scalar Mediator. Following the discussion of section III but working in the alternative frame of a fermionic dark matter (see Fig.(8)) particle interacting with the standard model via a scalar portal, one can write the following lagrangian

$$\mathcal{L}_{eff} = g_\chi \phi \bar{\chi}\chi + \frac{\phi}{\Lambda} F_{\mu\nu} F^{\mu\nu}.$$

One then gets the annihilation cross section

$$\langle\sigma v\rangle_{\gamma\gamma}^{micro} = \frac{2g_\chi^2 m_\chi^4 v^2}{\pi\Lambda^2(4m_\chi^2 - m_\phi^2)^2}. \quad (33)$$

which in what follows is fixed in order to fit the X-ray monochromatic signal.

Furthermore, one can still differentiate between the two cases where the mass of the mediator is heavier or lighter than the dark matter one.

Case A : $m_\phi \gtrsim m_\chi$ (Heavy Mediator)

$$m_\phi \simeq (0.97 - 1.4) \left(\frac{2g_\chi^2 v^2}{\pi} \right)^{1/4} \left(\frac{m_\chi}{3.5 \text{ keV}} \right) \sqrt{\frac{1 \text{ TeV}}{\Lambda}} \text{ MeV} \quad (34)$$

Case B : $m_\phi \lesssim m_\chi$ (Light Mediator)

$$\frac{g_\chi^2 v^2}{\Lambda^2} \sim 4.2 \times 10^{-14} \text{ GeV}^{-2} \quad (35)$$

The cross section is velocity suppressed here and leads, for a given value of the mediator mass and of the coupling

g_χ , to smaller values of the mass scale Λ . For example, for $g_\chi = 1$ in case B, one gets $\Lambda \sim 1.4 \times 10^6$ GeV.

Pseudo-Scalar Mediator. Another option is to make the dark sector communicate with the standard model through the exchange of a pseudo-scalar particle. The lagrangian is given by

$$\mathcal{L}_{eff} = g_\chi \phi \bar{\chi} \gamma_5 \chi + \frac{\phi}{\Lambda} F_{\mu\nu} \tilde{F}^{\mu\nu},$$

and the annihilation cross section is

$$\langle \sigma v \rangle_{\gamma\gamma}^{micro} = \frac{2g_\chi^2 m_\chi^4}{\pi \Lambda^2 (4m_\chi^2 - m_\phi^2)^2}, \quad (36)$$

which is now not velocity suppressed anymore.

Case A : $m_\phi \gtrsim m_\chi$ (Heavy Mediator)

$$m_\phi \simeq (0.97 - 1.4) \left(\frac{2g_\chi^2}{\pi} \right)^{1/4} \left(\frac{m_\chi}{3.5 \text{ keV}} \right) \sqrt{\frac{1 \text{ TeV}}{\Lambda}} \text{ MeV} \quad (37)$$

Case B : $m_\phi \lesssim m_\chi$ (Light Mediator)

$$\frac{g_\chi^2}{\Lambda^2} \sim 4.2 \times 10^{-14} \text{ GeV}^{-2} \quad (38)$$

In case B fitting the X-ray signal requires therefore $\Lambda \sim 5 \times 10^6$ GeV.

In both the cases of scalar and pseudo-scalar mediators, as is the case in the rest of the paper, case B is always excluded, regarding to the HB experimental bounds. As far as the Case A is concerned, the discussion is similar and g_χ plays the same role as \tilde{m} . However the needed values of Λ are different compared to the scalar dark matter : $\Lambda \lesssim 10$ TeV for Eq.(34) and $\Lambda \lesssim 100$ TeV for Eq.(37).

-
- [1] G. Hinshaw *et al.* [WMAP Collaboration], *Astrophys. J. Suppl.* **208** (2013) 19 [arXiv:1212.5226 [astro-ph.CO]].
- [2] P. A. R. Ade *et al.* [Planck Collaboration], arXiv:1303.5076 [astro-ph.CO].
- [3] E. Aprile *et al.* [XENON100 Collaboration], *Phys. Rev. Lett.* **109** (2012) 181301 [arXiv:1207.5988 [astro-ph.CO]].
- [4] D. S. Akerib *et al.* [LUX Collaboration], arXiv:1310.8214 [astro-ph.CO].
- [5] M. Ackermann *et al.* [Fermi-LAT Collaboration], *Phys. Rev. D* **89** (2014) 042001 [arXiv:1310.0828 [astro-ph.HE]]; M. Ackermann *et al.* [Fermi-LAT Collaboration], *Phys. Rev. D* **88** (2013) 082002 [arXiv:1305.5597 [astro-ph.HE]]; G. A. Gomez-Vargas, M. A. Sanchez-Conde, J. -H. Huh, M. Peiro, F. Prada, A. Morselli, A. Klypin and D. G. Cerdano *et al.*, arXiv:1308.3515 [astro-ph.HE].
- [6] L. J. Hall, K. Jedamzik, J. March-Russell and S. M. West, *JHEP* **1003** (2010) 080 [arXiv:0911.1120 [hep-ph]]. J. McDonald, *Phys. Rev. Lett.* **88** (2002) 091304 [hep-ph/0106249].
- [7] X. Chu, T. Hambye and M. H. G. Tytgat, *JCAP* **1205** (2012) 034 [arXiv:1112.0493 [hep-ph]]; C. E. Yaguna, *JCAP* **1202** (2012) 006 [arXiv:1111.6831 [hep-ph]]; X. Chu, Y. Mambrini, Jrm. Quevillon and B. Zaldivar, arXiv:1306.4677 [hep-ph]; A. Goudelis, Y. Mambrini and C. Yaguna, *JCAP* **0912** (2009) 008 [arXiv:0909.2799 [hep-ph]].
- [8] Y. Mambrini, K. A. Olive, J. Quevillon and B. Zaldivar, *Phys. Rev. Lett.* **110** (2013) 24, 241306 [arXiv:1302.4438 [hep-ph]].
- [9] A. Kusenko, *Phys. Rept.* **481** (2009) 1 [arXiv:0906.2968 [hep-ph]].
- [10] D. J. H. Chung, E. W. Kolb and A. Riotto, *Phys. Rev. Lett.* **81** (1998) 4048 [hep-ph/9805473]; D. J. H. Chung, E. W. Kolb and A. Riotto, *Phys. Rev. D* **60** (1999) 063504 [hep-ph/9809453]; E. W. Kolb, D. J. H. Chung and A. Riotto, In *Heidelberg 1998, Dark matter in astrophysics and particle physics 1998* 592-614 [hep-ph/9810361].
- [11] L. Dugger, T. E. Jeltema and S. Profumo, *JCAP* **1012** (2010) 015 [arXiv:1009.5988 [astro-ph.HE]].
- [12] E. Bulbul, M. Markevitch, A. Foster, R. K. Smith, M. Loewenstein and S. W. Randall, arXiv:1402.2301 [astro-ph.CO].
- [13] A. Boyarsky, O. Ruchayskiy, D. Iakubovskiy and J. Franse, arXiv:1402.4119 [astro-ph.CO].
- [14] See e.g. A. Boyarsky, O. Ruchayskiy and M. Shaposhnikov, *Ann. Rev. Nucl. Part. Sci.* **59** (2009) 191 [arXiv:0901.0011 [hep-ph]].
- [15] H. Ishida, K. S. Jeong and F. Takahashi, arXiv:1402.5837 [hep-ph]; K. N. Abazajian, arXiv:1403.0954 [astro-ph.CO]; F. Bezrukov and D. Gorbunov, arXiv:1403.4638 [hep-ph]; T. Tsuyuki, arXiv:1403.5053 [hep-ph]; K. P. Modak, arXiv:1404.3676 [hep-ph]; D. J. Robinson and Y. Tsai, arXiv:1404.7118 [hep-ph].
- [16] T. Higaki, K. S. Jeong and F. Takahashi, arXiv:1402.6965 [hep-ph]; J. Jaeckel, J. Redondo and A. Ringwald, arXiv:1402.7335 [hep-ph]; H. M. Lee, S. C. Park and W. -I. Park, arXiv:1403.0865 [astro-ph.CO]; M. Cicoli, J. P. Conlon, M. C. D. Marsh and M. Rummel, arXiv:1403.2370 [hep-ph]; J. P. Conlon and F. V. Day, arXiv:1404.7741 [hep-ph].
- [17] K. Kong, J. -C. Park and S. C. Park, arXiv:1403.1536 [hep-ph]; K. -Y. Choi and O. Seto, arXiv:1403.1782 [hep-ph].
- [18] K. Nakayama, F. Takahashi and T. T. Yanagida, "X-ray line signal," arXiv:1403.7390 [hep-ph].
- [19] C. Kolda and J. Unwin, arXiv:1403.5580 [hep-ph]; N. -E. Bomark and L. Roszkowski, arXiv:1403.6503 [hep-ph].
- [20] S. V. Demidov and D. S. Gorbunov, arXiv:1404.1339 [hep-ph].
- [21] P. Ko, Z. kang, T. Li and Y. Liu, arXiv:1403.7742 [hep-ph].

- ph].
- [22] R. Krall, M. Reece and T. Roxlo, arXiv:1403.1240 [hep-ph].
 - [23] C. m. E. Aisati, T. Hambye and T. Scarna, arXiv:1403.1280 [hep-ph].
 - [24] J. M. Cline, Y. Farzan, Z. Liu, G. D. Moore and W. Xue, arXiv:1404.3729 [hep-ph].
 - [25] M. Khlopov, Int. J. Mod. Phys. A **28** (2013) 1330042 [arXiv:1311.2468 [astro-ph.CO]]; M. Y. .Khlopov, arXiv:1402.0181 [hep-ph].
 - [26] H. M. Lee, arXiv:1404.5446 [hep-ph].
 - [27] F. S. Queiroz and K. Sinha, arXiv:1404.1400 [hep-ph].
 - [28] R. Allahverdi, B. Dutta and Y. Gao, arXiv:1403.5717 [hep-ph].
 - [29] D. P. Finkbeiner and N. Weiner, arXiv:1402.6671 [hep-ph].
 - [30] H. Okada and T. Toma, arXiv:1404.4795 [hep-ph].
 - [31] M. R. Lovell, C. S. Frenk, V. R. Eke, A. Jenkins, L. Gao and T. Theuns, arXiv:1308.1399 [astro-ph.CO].
 - [32] M. Frandsen, F. Sannino, I. M. Shoemaker and O. Svendsen, arXiv:1403.1570 [hep-ph].
 - [33] R. Krall, M. Reece and T. Roxlo, arXiv:1403.1240 [hep-ph].
 - [34] T. Lin, H. -B. Yu and K. M. Zurek, Phys. Rev. D **85** (2012) 063503 [arXiv:1111.0293 [hep-ph]]; S. Galli, F. Iocco, G. Bertone and A. Melchiorri, Phys. Rev. D **84** (2011) 027302 [arXiv:1106.1528 [astro-ph.CO]].
 - [35] K. Belotsky, A. Kirillov and M. Khlopov, Grav. Cosmol. **20** (2014) 47 [arXiv:1212.6087 [astro-ph.HE]].
 - [36] C. Boehm and P. Fayet, Nucl. Phys. B **683** (2004) 219 [hep-ph/0305261].
 - [37] C. Boehm, T. A. Ensslin and J. Silk, J. Phys. G **30** (2004) 279 [astro-ph/0208458].
 - [38] J. Goodman, M. Ibe, A. Rajaraman, W. Shepherd, T. M. P. Tait and H. -B. Yu, Phys. Rev. D **82** (2010) 116010 [arXiv:1008.1783 [hep-ph]].
 - [39] P. J. Fox, R. Harnik, J. Kopp and Y. Tsai, Phys. Rev. D **84** (2011) 014028 [arXiv:1103.0240 [hep-ph]]; Y. Mambrini and B. Zaldivar, JCAP **1110** (2011) 023 [arXiv:1106.4819 [hep-ph]]; H. Dreiner, M. Huck, M. Krmer, D. Schmeier and J. Tattersall, Phys. Rev. D **87** (2013) 7, 075015 [arXiv:1211.2254 [hep-ph]]; K. Cheung, P. -Y. Tseng, Y. -L. S. Tsai and T. -C. Yuan, JCAP **1205** (2012) 001 [arXiv:1201.3402 [hep-ph]].
 - [40] M. Papucci, A. Vichi and K. M. Zurek, arXiv:1402.2285 [hep-ph].
 - [41] X. Chu, T. Hambye, T. Scarna and M. H. G. Tytgat, Phys. Rev. D **86** (2012) 083521 [arXiv:1206.2279 [hep-ph]].
 - [42] Cl. Boehm, M. J. Dolan and C. McCabe, JCAP **1308**, 041 (2013) [arXiv:1303.6270 [hep-ph]].
 - [43] A. Rajaraman, T. M. P. Tait and A. M. Wijangco, Phys. Dark Univ. **2** (2013) 17 [arXiv:1211.7061 [hep-ph]].
 - [44] M. Pospelov, A. Ritz and M. B. Voloshin, Phys. Lett. B **662** (2008) 53 [arXiv:0711.4866 [hep-ph]].
 - [45] J. L. Feng, H. Tu and H. -B. Yu, JCAP **0810** (2008) 043 [arXiv:0808.2318 [hep-ph]]; S. Das and K. Sigurdson, Phys. Rev. D **85** (2012) 063510 [arXiv:1012.4458 [astro-ph.CO]].
 - [46] M. Kleban and R. Rabadan, hep-ph/0510183.
 - [47] G. G. Raffelt, Chicago, USA: Univ. Pr. (1996) 664 p
 - [48] J. L. Hewett, H. Weerts, R. Brock, J. N. Butler, B. C. K. Casey, J. Collar, A. de Gouvea and R. Essig *et al.*, arXiv:1205.2671 [hep-ex].
 - [49] R. Essig, R. Harnik, J. Kaplan and N. Toro, Phys. Rev. D **82** (2010) 113008 [arXiv:1008.0636 [hep-ph]].
 - [50] J. L. Hewett, H. Weerts, R. Brock, J. N. Butler, B. C. K. Casey, J. Collar, A. de Gouvea and R. Essig *et al.*, arXiv:1205.2671 [hep-ex].
 - [51] M. Frigerio and T. Hambye, Phys. Rev. D **81** (2010) 075002 [arXiv:0912.1545 [hep-ph]].
 - [52] R. Slansky, Phys. Rept. **79** (1981) 1.
 - [53] T. Fukuyama, A. Ilakovac, T. Kikuchi, S. Meljanac and N. Okada, J. Math. Phys. **46** (2005) 033505 [hep-ph/0405300].
 - [54] S. Das and K. Sigurdson, Phys. Rev. D **85** (2012) 063510 [arXiv:1012.4458 [astro-ph.CO]].
 - [55] J. L. Feng, H. Tu and H. -B. Yu, JCAP **0810** (2008) 043 [arXiv:0808.2318 [hep-ph]].
 - [56] S. Tremaine and J. E. Gunn, Phys. Rev. Lett. **42** (1979) 407.
 - [57] . Bolz, A. Brandenburg and W. Buchmuller, Nucl. Phys. B **606** (2001) 518 [Erratum-ibid. B **790** (2008) 336] [hep-ph/0012052]; V. S. Rychkov and A. Strumia, Phys. Rev. D **75** (2007) 075011 [hep-ph/0701104].
 - [58] G. F. Giudice, A. Notari, M. Raidal, A. Riotto and A. Strumia, Nucl. Phys. B **685** (2004) 89 [hep-ph/0310123]; S. Antusch and A. M. Teixeira, JCAP **0702** (2007) 024 [hep-ph/0611232].
 - [59] S. Davidson and A. Ibarra, Phys. Lett. B **535** (2002) 25 [hep-ph/0202239]; E. Nardi, Y. Nir, E. Roulet and J. Racker, JHEP **0601** (2006) 164 [hep-ph/0601084]; A. Abada, S. Davidson, A. Ibarra, F. -X. Josse-Michaux, M. Losada and A. Riotto, JHEP **0609** (2006) 010 [hep-ph/0605281]; R. Barbieri, P. Creminelli, A. Strumia and N. Tetradis, Nucl. Phys. B **575** (2000) 61 [hep-ph/9911315]; M. Raidal, A. Strumia and K. Turzynski, Phys. Lett. B **609** (2005) 351 [Erratum-ibid. B **632** (2006) 752] [hep-ph/0408015]; A. Pilaftsis and T. E. J. Underwood, Nucl. Phys. B **692** (2004) 303 [hep-ph/0309342].